NAVAL POSTGRADUATE SCHOOL

MONTEREY, CALIFORNIA

THESIS

POWER CONDITIONING FOR MEMS-BASED WASTE VIBRATIONAL ENERGY HARVESTER

by

Seyfullah Emen

June 2015

Thesis Advisor:	Dragoslav Grbovic
Co-Advisor:	Sherif Michael

Approved for public release; distribution is unlimited

THIS PAGE INTENTIONALLY LEFT BLANK

REPORT DOCUMENTATION PAGE

Form Approved OMB No. 0704–0188

1. AGENCY USE ONLY *(Leave blank)*	2. REPORT DATE June 2015	3. REPORT TYPE AND DATES COVERED Master's Thesis

4. TITLE AND SUBTITLE POWER CONDITIONING FOR MEMS-BASED WASTE VIBRATIONAL ENERGY HARVESTER	5. FUNDING NUMBERS
6. AUTHOR(S) Seyfullah Emen	

7. PERFORMING ORGANIZATION NAME(S) AND ADDRESS(ES) Naval Postgraduate School Monterey, CA 93943-5000	8. PERFORMING ORGANIZATION REPORT NUMBER

9. SPONSORING /MONITORING AGENCY NAME(S) AND ADDRESS(ES) N/A	10. SPONSORING/MONITORING AGENCY REPORT NUMBER

11. SUPPLEMENTARY NOTES The views expressed in this thesis are those of the author and do not reflect the official policy or position of the Department of Defense or the U.S. Government. IRB Protocol number ____N/A____.

12a. DISTRIBUTION / AVAILABILITY STATEMENT Approved for public release; distribution is unlimited	12b. DISTRIBUTION CODE A

13. ABSTRACT (maximum 200 words)

Increasing energy needs push industry to build more sustainable and efficient systems. One of the methods to achieve energy efficiency is to feed wasted energy generated by a system itself during operation back to the system. Vibrational energy is one of the most common ambient energy forms in mechanical systems and can be converted into electrical energy with the implementation of piezoelectric energy harvesters. What makes this possible is the piezoelectric effect that some crystals and ceramics with no inversion symmetry show. Piezoelectric materials generate a potential difference when a force is applied and deform under an electric field. Power electronics is used to turn this potential into a usable energy.

The amount of power generated by a single piezoelectric energy harvester could be very low, but Microelectromechanical Systems (MEMS) technology makes it possible to have thousands of devices in a very small area. Previously, a MEMS-based piezoelectric harvester for military applications was designed, developed, and tested at NPS. In this thesis, methods to convert the AC voltage output of this device into a DC voltage were investigated to find an efficient method. Because of their higher power needs, multiple devices need to be connected to achieve required power levels for military applications. Microfabrication processes allow for building large number of such devices at the same time. This thesis also studies the possible connections for an array of devices. Connection geometry that will produce the maximum power output for a number of devices is proposed.

14. SUBJECT TERMS MEMS, Waste Energy Harvesting, Piezoelectric, Power Conditioning, Piezoelectric Energy Harvester	15. NUMBER OF PAGES 53
	16. PRICE CODE

17. SECURITY CLASSIFICATION OF REPORT Unclassified	18. SECURITY CLASSIFICATION OF THIS PAGE Unclassified	19. SECURITY CLASSIFICATION OF ABSTRACT Unclassified	20. LIMITATION OF ABSTRACT UU

NSN 7540–01-280-5500

Standard Form 298 (Rev. 2–89)
Prescribed by ANSI Std. 239–18

THIS PAGE INTENTIONALLY LEFT BLANK

POWER CONDITIONING FOR MEMS-BASED WASTE VIBRATIONAL ENERGY HARVESTER

Seyfullah Emen
Lieutenant Junior Grade, Turkish Navy
B.S., Turkish Naval Academy, 2010

Submitted in partial fulfillment of the
requirements for the degree of

MASTER OF SCIENCE IN PHYSICS

from the

**NAVAL POSTGRADUATE SCHOOL
June 2015**

Author: Seyfullah Emen

Approved by: Dragoslav Grbovic
               Thesis Advisor

               Sherif Michael
               Co-Advisor

               Andres Larraza
               Chair, Department of Physics

THIS PAGE INTENTIONALLY LEFT BLANK

ABSTRACT

Increasing energy needs push industry to build more sustainable and efficient systems. One of the methods to achieve energy efficiency is to feed wasted energy generated by a system itself during operation back to the system. Vibrational energy is one of the most common ambient energy forms in mechanical systems and can be converted into electrical energy with the implementation of piezoelectric energy harvesters. What makes this possible is the piezoelectric effect that some crystals and ceramics with no inversion symmetry show. Piezoelectric materials generate a potential difference when a force is applied and deform under an electric field. Power electronics is used to turn this potential into a usable energy.

The amount of power generated by a single piezoelectric energy harvester could be very low, but Microelectromechanical Systems (MEMS) technology makes it possible to have thousands of devices in a very small area. Previously, a MEMS-based piezoelectric harvester for military applications was designed, developed, and tested at NPS. In this thesis, methods to convert the AC voltage output of this device into a DC voltage were investigated to find an efficient method. Because of their higher power needs, multiple devices need to be connected to achieve required power levels for military applications. Microfabrication processes allow for building large number of such devices at the same time. This thesis also studies the possible connections for an array of devices. Connection geometry that will produce the maximum power output for a number of devices is proposed.

THIS PAGE INTENTIONALLY LEFT BLANK

TABLE OF CONTENTS

THIS PAGE INTENTIONALLY LEFT BLANK

LIST OF FIGURES

THIS PAGE INTENTIONALLY LEFT BLANK

LIST OF TABLES

THIS PAGE INTENTIONALLY LEFT BLANK

LIST OF ACRONYMS AND ABBREVIATIONS

AC	Alternative Current
AlN	Aluminum Nitride
DC	Direct Current
LIA	Lock-In Amplifier
MEMS	Microelectromechanical Systems
MOSFET	Metal-oxide-semiconductor Field-effect Transistor
PEH	Piezoelectric Energy Harvester
PiezoMUMPS	Piezoelectric Multi-User MEMS Processes

THIS PAGE INTENTIONALLY LEFT BLANK

ACKNOWLEDGMENTS

First of all, a very special thanks to my advisor Dr. Dragoslav Grbovic. Without his knowledge, time, and assistance, this thesis would not have been possible.

I would like express my sincere gratitude to Professors Sherif Michael and Fabio Alves and to LCDR Timothy J. Householder for their guidance. I also thank Matthew Porter for his remarks and comments and Steven Jacobs for his help.

THIS PAGE INTENTIONALLY LEFT BLANK

I. INTRODUCTION

Energy efficiency is a key concept in systems. One of the methods to achieve energy efficiency is to scavenge the wasted energy generated by the system itself during operation. That wasted energy could be thermal, acoustic, vibrational, or radio frequency according to the type of system. In mechanical systems, vibrational energy is one of the most common ambient energy forms, and can be converted into electrical energy with the implementation of piezoelectric energy harvesters (PEHs). Whether with a single device or an array of devices according to the power requirement, recapturing ambient vibrations can increase the efficiency of an engine, create self-sufficient systems, and provide a clean energy solution.

This thesis continues the work of "MEMS-based waste vibration and acoustic energy harvesters" performed by Timothy Householder [1] and "MEMS-based waste vibrational energy harvesters" Sarah Gregory and Daniel Hogue [2]. In his thesis, Householder [1] successfully developed and tested a PEH for which the main design and fabrication steps were described in the previous thesis [2]. In this thesis, a second device is developed and tested, an equivalent model for the device is produced, power conditioning circuitry for the optimum power output is investigated and different connection geometries for a number of devices were tested to get maximum power output.

A. PIEZOELECTRICITY

Some crystals or ceramics with no inversion symmetry generate a potential difference when a force is applied, or deform under an electric field [3]. Origin of this effect is the displacement of ionic charges within the crystal that results in an electric field inside the material [4]. In this thesis, the direct piezoelectric effect (conversion of mechanical force into electrical energy) is studied. The general equation that expresses the relationship between electric displacement (D), applied mechanical stress (T), and electric field (E) is

$$D = dT + \varepsilon E \tag{1}$$

1

where d and ε are the piezoelectric coefficient and electrical permittivity, respectively. If no electric field is applied (E=0), (1) becomes

$$D = dT \qquad\qquad (2)$$

Equation (2) is the governing equation for direct piezoelectric effect.

B.   PREVIOUS WORK

Modeled with COMSOL and designed with MEMSPro software packages, the device in Figure 1 was tested and its characteristics were determined by [1]. Aluminum nitride (AlN) was chosen as the piezoelectric material for its high piezoelectric modulus, low cost, and compatibility with microfabrication processes.
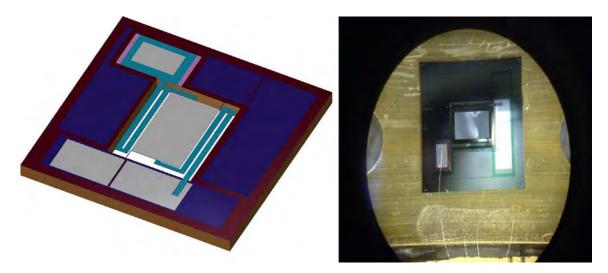
Figure 1.   Device designed and tested by Householder, from [1]

Householder mechanically tested the device for range of frequencies with the setup in Figure 2. The same setup will be used in this thesis.
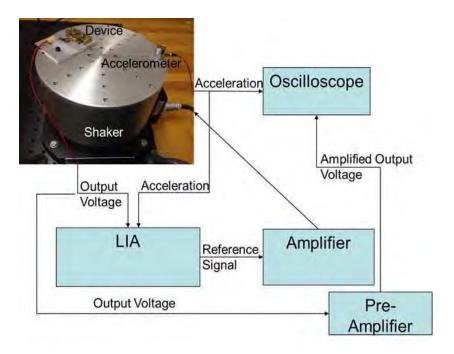
Figure 2.   Vibrational test setup, from [1]

According to the test results, the device has a resonance peak at 380 Hz for 200 mV$_{rms}$ constant accelerometer voltage. Considering SRS-850 DSP Lock-In Amplifier (LIA) and Tektronix DPO 2012 Digital Oscilloscope as electric load, his output power estimation is in Table 1.

Table 1.   Power estimation, from [1]

	Voltage (mV$_{rms}$)	Frequency (Hz)	Impedance (MΩ)	Power (fW)
Lock-In Amplifier	0.221	379.3	52.7	0.924
Oscilloscope	4.8	380.5	36.4	633.0

Since the power depends on the load, the difference between two different measuring devices can be several orders of magnitude because of the difference between internal impedances. For the optimum power output, the load impedance needs to match the impedance of the device [3]. This is explained in Chapter III.

THIS PAGE INTENTIONALLY LEFT BLANK

II.   EQUIVALENT MODEL

In order to investigate power output, power conditioning methods, and behaviors of a single or an array of PEHs, it is necessary to come up with a model.

A.   MECHANICAL MODEL

Developed by Williams and Yates [5] and explained in [3], a PEH can be mechanically modeled as a spring-mass system shown in Figure 3, with k_s, m, z(t), y(t), d, and F_e being stiffness of the spring, mass, mass position, frame position, damping and restoring force, respectively.
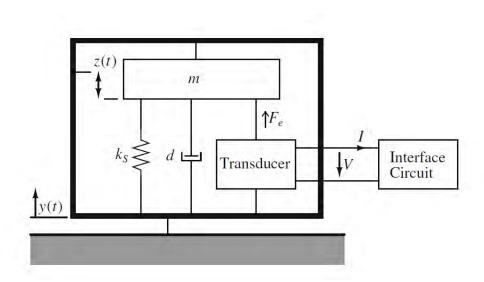
Figure 3.   Mechanical equivalent model of a PEH, from [3]

B.   ELECTRICAL MODEL

A mechanical model helps us to understand the physics of the harvester. Since this thesis studies the electrical aspect of the harvester, an electrically equivalent circuit is needed to estimate the power output of a single or an array of devices.

Basically a PEH is an RLC circuit [3]. Figure 4 shows the equivalent circuit with parameters represented in terms of parameters of the mechanical model in Figure 3.
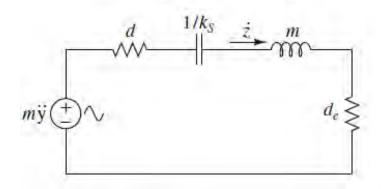
Figure 4.   Electrical equivalent model of a PEH as an RLC circuit, from [3]

In a case like ours, where we are interested in the optimal connection of multiple devices, all operating at resonant frequency, a simpler, purely electrical equivalent model can be used to simulate the multi-device behavior. A simplified model, used to investigate output under different loads, is shown in Figure 5. In this model, mechanical and electrical systems are decoupled, and the device is modeled as a Thévenin equivalent circuit that consists of a voltage source and internal impedance connected in a series [7] as in Figure 5. Impedance measurement is made in Chapter III.
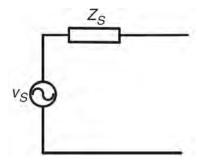
Figure 5.   Simplified electrical equivalent circuit, from [7]

III.   SECOND DEVICE

To do further tests and possible connection combinations in series and in parallel, a second device was prepared. The third generation PiezoMUMPs design in Figure 1 was used. After removal from the shipping tape, the thickness of the layers was measured using Zygo NanoView 7100 Optical Profilometer and Filmetrics spectroscopic thickness measurement instrument. The thickness comparison of the two devices is shown in Table 2.

Table 2.   Thicknesses of first and second devices

	Structure (Si)		Piezo (AlN)		Pad Metal (Al)	
	1st Device	2nd Device	1st Device	2nd Device	1st Device	2nd Device
Optical Profilometer	10.1 μm		498.9 nm	503.9 nm	0.99 μm	1.03 μm
Filmetrics	-	-	493.2 nm	489.3 nm	-	-
Design	10 μm		500 nm		1.02 μm	

The devices were obtained through a commercial foundry PiezoMUMPS, as a part of a group that was testing their new process. As such, the across-the-wafer uniformity was not optimal. Even though they were diced from the same wafer there is an apparent difference between thicknesses of two dies as well as the stress levels. When a 3D profile of two devices is taken with the Zygo optical profilometer, it is apparent that the legs are stress-deformed differently as shown in Figure 6. This implies that the stress on the second device is different than the first one. Such differences can influence the resonance frequency and mode, and may be the reason for difference in behavior of devices.
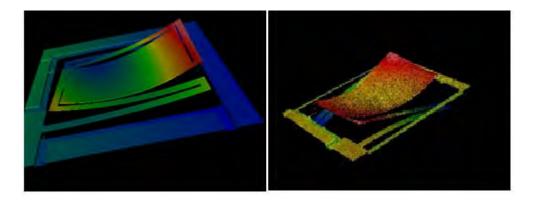
Figure 6.   Optical profilometer image of first (left) and second (right) devices

To prepare the device for mechanical and electrical tests, wire bonding was made using K&S 4524A Digital Bonder. During wire bonding, it was realized that the aluminum layer on the device was oxidized, which made the wire bonding process more difficult. For future work, it is recommended to put the die in oxygen plasma to remove the oxide layer before measurements and wire bonding.

Another difference between the two devices is the thickness of the aluminum plate used as a foundation. Since the wire bonder has limitations in z direction, for easier wire bonding, we used a thinner aluminum plate as shown in Figure 7. Note that the voltage output of the device changes according to the point device is anchored to the shaker. Instead of the thin aluminum plate, the device should be anchored to the shaker from one of the points on the brass section.
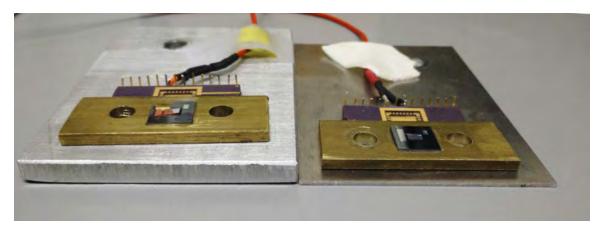
Figure 7.   First (left) and second (right) PEHs

A.   MECHANICAL TEST

Using the same setup in Figure 2 and previous settings [1], the second device was tested. The signal created by the LIA was sent to the APS model 114 Dual-Mode Power Amplifier, which drives the APS Model 120S Perma-Dyne Shaker that simulates the ambient vibration to test the device mechanically. The output of the energy harvester device and Endevco Isoshear Model 7701A-100 Accelerometer was read by the LIA and monitored by the Tektronix DPO 2012 Digital Oscilloscope. Previously [1], device output was amplified by SRS Model SR560 Low Noise Preamplifier before being fed into the oscilloscope. However, this time the output signal was strong and clean enough to measure in the oscilloscope, so the preamplifier is taken out of the experimental setup in Figure 2.

1.   Output Voltage

For a vibrational sweep from 100 Hz to 1 kHz, the output of the device is measured. To factor out minor variations in output, the same normalization method [1] is used. Equations (3) and (4) show the normalization method used for both device outputs.

$$V = \frac{V_{out}}{V_{acc}} \qquad\qquad\qquad (3)$$

$$\theta = \theta_{out} - \theta_{acc} \qquad\qquad\qquad (4)$$

Where V_{out} and V_{acc} are output voltages for the device and accelerometer; θ_{out} and θ_{acc} are the phase angles of the device and accelerometer.

Figure 8 shows the output of the two devices.
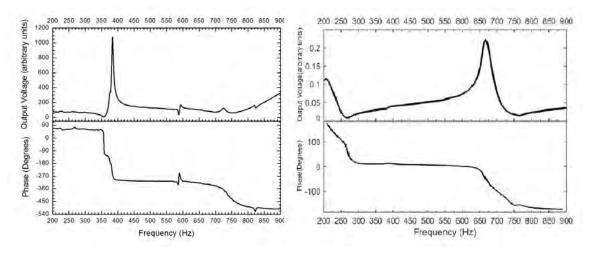
Figure 8.   Normalized voltage output and phase of first (left) and second (right) devices

Resonance peak of the first device was measured as 380 Hz; however in the second device we have a higher resonance peak which is 665 Hz according to the LIA. Also the output voltage of the second device is higher.

To further investigate the resonance peak at 665 Hz, a manual frequency sweep done, and the output voltage was read with the oscilloscope and a Fluke 85 III True RMS Multimeter. Figure 9 shows the plots. Resonance frequency was determined to be 665 Hz, 661 Hz and 660 Hz by the LIA, oscilloscope, and multimeter, respectively.
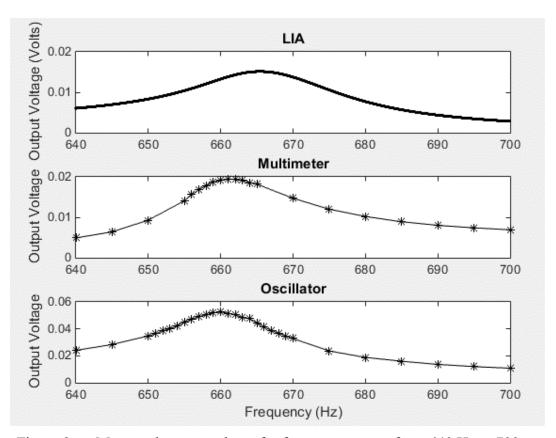
Figure 9. Measured output voltage for frequency sweep from 640 Hz to 700 Hz by LIA, multimeter, and oscilloscope

2. Power Estimation

The input resistance of the LIA is 10 MΩ with a 25pF capacitance whereas the oscilloscope has 1MΩ resistance with 11.5 pF capacitance. Resonance frequencies measured by the LIA and oscilloscope are 665 Hz and 660 Hz respectively. Since the impedance for a resistor and capacitor in series is

$$|Z| = \sqrt{R^2 + X_c^2} = \sqrt{R^2 + \frac{1}{(2\pi f C)^2}} \qquad (5)$$

impedances of the LIA and oscilloscope will be 13.84MΩ and 20.96MΩ, respectively.

The measured output voltages in resonance frequencies are 15 mV$_{rms}$ on the LIA and 37 mV$_{rms}$ on the oscilloscope. Since power is

$$P = \frac{V^2}{R} \qquad (6)$$

11

The power provided to the LIA and oscilloscope will be 16.3 pW and 65.2 pW, respectively. The large difference between these values and the estimated power in Householder's work [1] is mainly because of higher voltage output and resonance frequency.

B.   IMPEDANCE MEASUREMENT

Impedance in a circuit is the opposition to the flow of the current. It can be represented as

$$Z = R + jX \qquad (7)$$

For R as resistance and X as reactance (capacitive or inductive according to the circuit or device). To determine the impedance of the device, Quad Core 7600 RLC meter is used. For a frequency sweep from 640 Hz to 680 Hz for 0.4 mV input, impedance and phase angle values are shown in Figure 10.
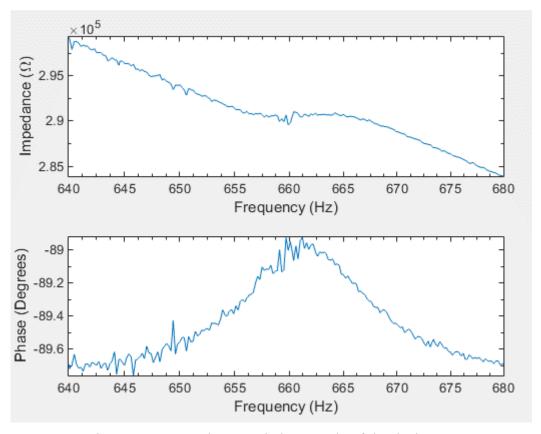
Figure 10.   Impedance and phase angle of the device

12

We can see that the resonance frequency peaks at 660.1 Hz. Resonance frequencies were measured as 661 Hz, 660 Hz and 665 Hz by multimeter, oscilloscope and LIA, respectively.

In Quad Core 7600 RLC meter measurements, impedance of the device is represented as an equivalent circuit which consists of a resistance and a reactance connected in series or in parallel according to the nature of reactance. For a frequency sweep from 10 Hz to 1 kHz, we can fit the reactance of 828pF capacitor to the impedance curve as in Figure 11.

Both from phase and the impedance curve we can deduce that our PEH is capacitive. Figure 12 shows the series equivalent circuit and phase diagram of the impedance [6].
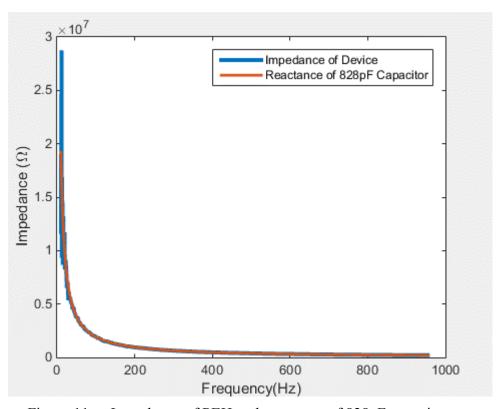
Figure 11.   Impedance of PEH and reactance of 828pF capacitor
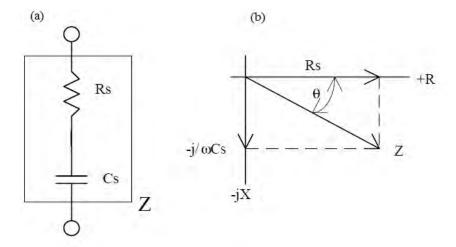
Figure 12.   Series circuit for capacitive impedance (a) and phase diagram of impedance (b), from [6]

We can measure R_S and C_S in Figure 12(a) with the RLC meter. For resonance frequency of 660.1 Hz, Rs and Cs are measured as 4924 Ω and 828.4 pF, respectively.

Capacitance value of the device is pretty high. From (5) we can see that reactance is dominant in impedance value. Figure 14 shows how reactance of the PEH fits the impedance. For simplification, we can exclude Rs in out equivalent circuit.
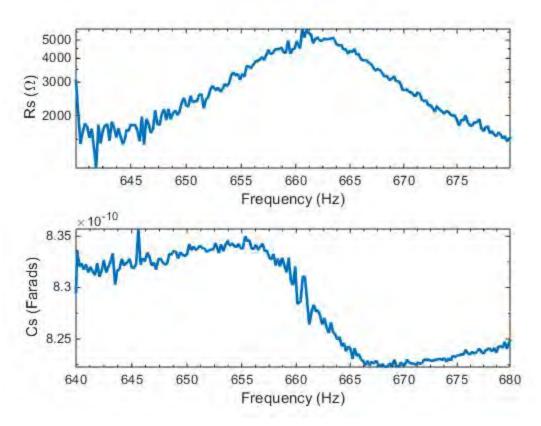
Figure 13.   Resistance (Rs) and capacitance (Cs) of PEH

After excluding R_s, the equivalent circuit in Figure 5 is simplified as a voltage source and a capacitor and shown in Figure 15.
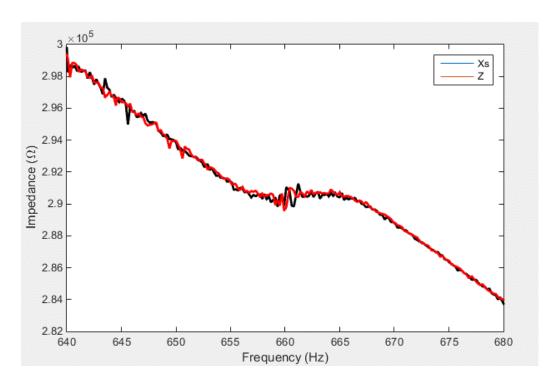
Figure 14.   Impedance (Z) and reactance (Xs) of PEH
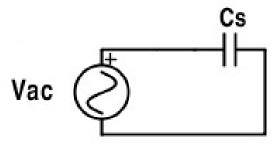
Figure 15.   Simplified equivalent circuit of PEH

C.   CONDITIONING CIRCUIT

In this section, the need for power conditioning is explained. Several conditioning methods are investigated for their suitability for our device and a power conditioning method is proposed.

A power conditioning circuit is necessary to obtain an efficient energy transfer between a harvester and the electric load [8]. According to the operating conditions,

16

power needs, and application, power conditioning circuits for energy harvesters vary. Power conditioning circuits for different needs and applications are investigated and compared in previous studies [9]–[12]. A standard power conditioning circuit consists of a rectifier and a load is shown in Figure 16. Components of the circuit are explained in more detailed way.

Figure 16.   Standard power conditioning circuit

Output of a piezoelectric harvester is an AC signal that must be converted into a DC signal to supply power to the load. Rectification circuits are used to convert AC into DC. This is generally realized by a rectifier circuit and a smoothing capacitor. Rectifier circuits could be active or passive. While passive rectifiers do not need any external power, active rectifiers require an external switching or triggering thus external power. Active rectifiers have higher efficiency but are comparatively more expensive and complicated than passive rectifiers. Since each PEH needs rectification and an array of thousands of devices will be microfabricated, active rectifiers will increase the cost and complexity of a single device or a piezoelectric energy harvester array that consists of thousands of devices. So, we will implement a passive rectifier for power conditioning. Defining the efficiency of the rectification η as ratio of DC output voltage V_{DC} and AC input voltage V_{AC}

$$\eta = \frac{V_{DC}}{V_{AC}} 100\% \tag{8}$$

Implementing the most efficient method is the key goal.

Voltage output of our device is 19 mV, which makes passive rectification impractical as this is quite below standard threshold voltages. To make the device more

17

applicable, its voltage output needs to be increased. Methods explained below are for future work.

One of the common methods of AC voltage rectification is using diodes. Figure 17 shows common diode rectification circuits.
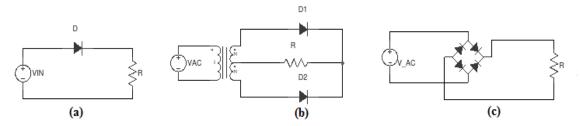
Figure 17.   Half-wave rectifier (a), full-wave rectifier (b) and full-wave bridge rectifier (c) circuits

For ultra-low voltage applications like ours, the main loss during rectification takes place within the diodes. The forward voltage drop of a silicon diode is around 0.7 V. In a full-wave bridge rectifier, diodes cause a 1.4 V voltage drop. Using germanium diodes will decrease the voltage drop to 0.3 V for a full bridge rectifier, but germanium diodes are more expensive than silicon diodes. Schottky diodes are another type of diode that can be used in rectifier circuits. Apart from being relatively expensive, their 0.1–0.3 V forward voltage drop still makes them insufficient low voltage applications [13]. Rectifiers using Schottky diodes becomes efficient ($\eta > 50\%$) for voltages over 0.7 V, whereas for silicon diode rectifiers efficiency is achieved when input voltage is over 2–3 V [14].

Using metal-oxide-semiconductor field-effect transistors (MOSFETs) in a rectifier instead of diodes help us get over the high forward voltage drop. Figure 18 shows a full-wave bridge rectifier with two N-type and two P-type MOSFETs.
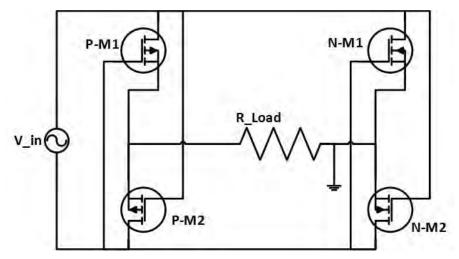
Figure 18.   Full-wave passive MOSFET rectifier circuit, from [14]

Whereas rectifiers with Schottky diodes are more efficient for lower voltages, for voltages over 0.8 V a full-wave passive MOSFET bridge rectifier reaches to 99% efficiency [14].

THIS PAGE INTENTIONALLY LEFT BLANK

IV.   POWER ANALYSIS

PEHs usually have very high internal impedance which results in low current even though they generate high voltages. In Chapter III, a power estimation of the device was made for considering internal impedance of the LIA and oscilloscope as the load. However, the power can be optimized by matching the load with the impedance of the device.

In this chapter, the maximum power output of a single device and an array of devices in different connection combinations are simulated using LTSPICE IV simulation software.

A.   SINGLE DEVICE

A LTSPICE model of the harvester used in the power estimation is shown in Figure 19.
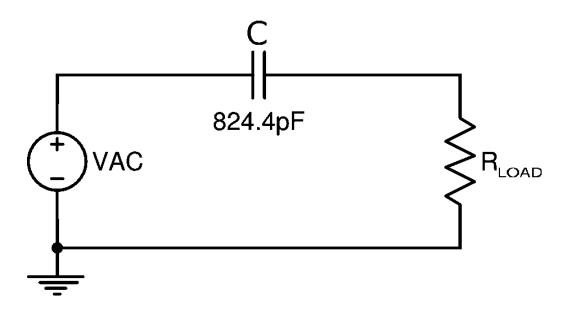
Figure 19.   PSPICE model of the PEH

As measured in Chapter III, the internal impedance of the device is around 290 kΩ. To simplify the circuit we neglect the resistance that makes the impedance of the

device equal to the reactance of the 828.4 pF capacitor which is 291 kΩ. We expect to have the maximum power when R_{LOAD} equals to 291 kΩ.

Figure 20 shows the voltage and power output of the model under loads from 1 kΩ to 100 MΩ.
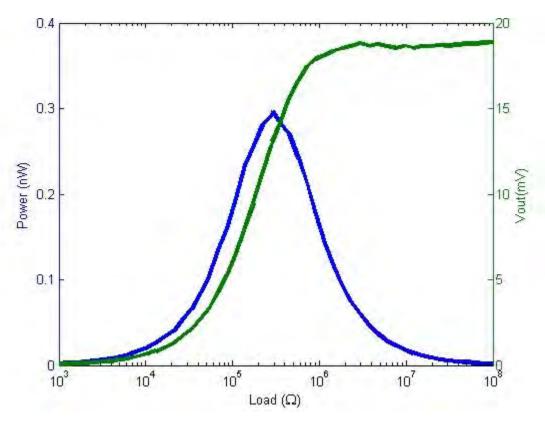
Figure 20.   Power and output voltage under different loads

We get the maximum power for R_{Load}=289.8 kΩ as 0.3nW as predicted. However, this power is very low for applications. In order to increase the power, we need to connect multiple devices in series or in parallel.

B.   MULTIPLE DEVICES

Devices are connected in series and parallel to see the change in the output. Measurements of power, voltage, and current were made after adding another device to the circuit. Figure 21 shows 12 PEHs connected in parallel and Figure 23 shows devices connected in series. Note that for each measurement, the load is matched with the

22

equivalent impedance of the devices in order to achieve the maximum power output. Voltage and current are also measured after impedance matching.
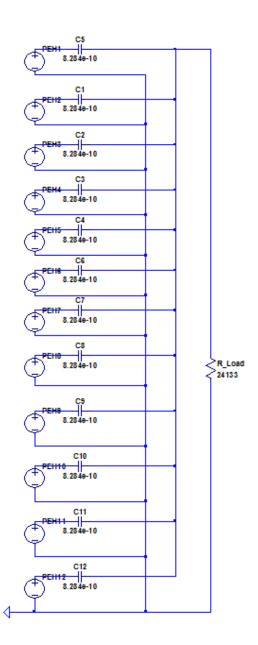
Figure 21.　Twelve PEHs connected in parallel

1.　Devices in Parallel

Figure 22 shows the results for devices connected in parallel. As we see the load decreases, voltage stays the same as both power and current increase linearly. To increase

the current, we need to connect more devices in parallel. The maximum power we get from 12 devices connected in parallel is 3.72 nW.
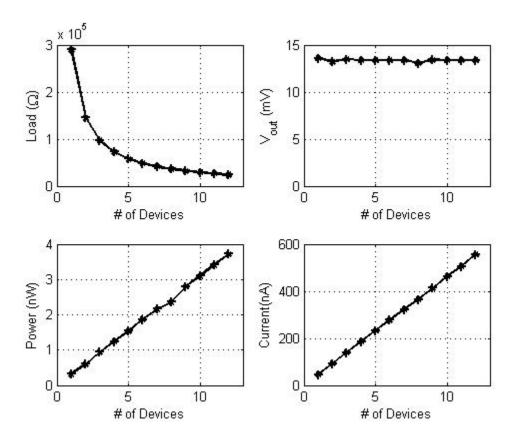
Figure 22.   Matched load, output voltage, power, and current of devices connected in parallel

2.   Devices in Series

Results of the measurements for connection in series are shown in Figure 24. Load, output voltage, and power increase as current stays the same. The maximum power we obtain from 12 devices connected in series is 3.68 nW, which is very close to maximum power in parallel connection.
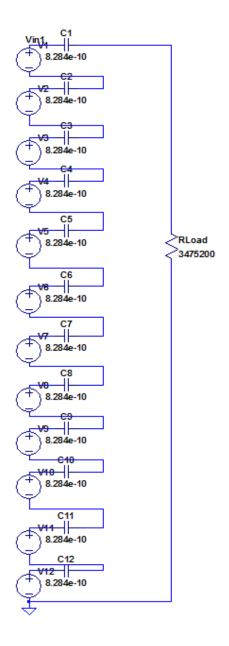
Figure 23.   Twelve PEHs connected in series
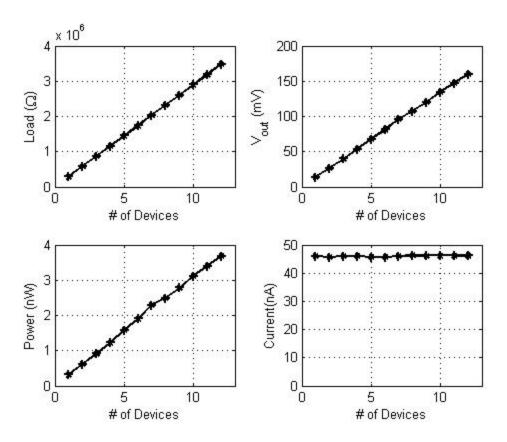
Figure 24.   Matched load, output voltage, power, and current of devices
connected in series

3.   Parallel and Series Connection

We have showed the behavior of devices when connected in series or in parallel. Voltage increases as more devices are connected in series, whereas current stays the same and vice versa for parallel connection. In order to achieve more applicable current and voltage levels, we need to connect devices both in parallel and in series at the same time. To investigate the optimum connection geometry, 12 devices are connected in different parallel and series combinations.

From Figure 25, we can see that power delivered to load for different combinations of 12 devices is almost the same. The reason for the small difference is calculation sensitivity. The same measurements were made for more devices, and the maximum power delivered to load stays same as output voltage and current changes according to the connection.

26
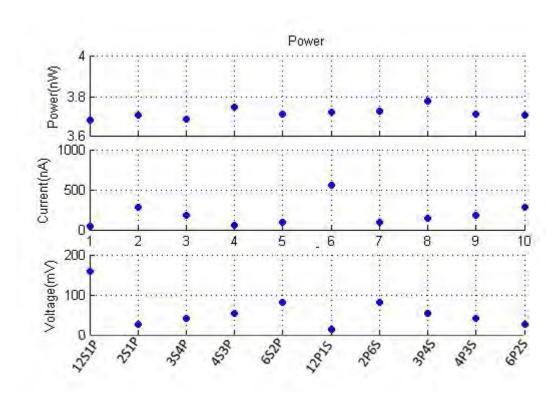
Figure 25.   Power, current, and voltage calculations of 12 devices connected in series and in parallel

THIS PAGE INTENTIONALLY LEFT BLANK

V. CONCLUSION AND FUTURE WORK

A second device equivalent to the one used in precious work [1] was mechanically tested for its electrical characteristics and an equivalent electrical model is produced for simulation. Components of a power conditioning circuit to convert AC output of the device to a stable DC voltage were explained. Using the electrical model power output of a single device was studied under different loads to find the maximum power delivered to a load. Finally, different connection geometries were studied to find the optimum connection for the maximum power output from an array of devices.

A.   CONCLUSION

Maximum output voltage of a single device is 19 mV which makes an efficient AC-DC conversion impractical for a single device. The voltage output of the device needs to be increased to 0.5–0.7 V to make the device more efficient according to the rectification method used. From the governing equation for the direct piezoelectric effect shown in (1) the output voltage is related to the z component of the electrical displacement [2]

$$V = \frac{D_3 t}{\varepsilon} \tag{9}$$

thus by increasing the thickness of the piezoelectric material (t), higher output voltages can be achieved.

As demonstrated and explained in Chapter IV, voltage, current, and therefore the power need to be increased for practical use. By connecting devices in parallel, the current increases; by adding devices in series, the output voltage increases. Connecting multiple devices together is one of the main drivers for this approach as microfabrication processes allow building large numbers of such devices at the same time.

For preferred power values, the number of devices can be determined and connections can be made according to the voltage and current needs. Note that this simulation was made for AC output considering all devices are in phase. However, this is

not practical for a large number of devices. Connections need to be made after AC-DC conversion.

B.   FUTURE WORK

Broad future work recommendations on different topics were previously made by Householder [1]. Recommendations on modeling, fabrications, and modal analysis remain valid.

Most of the recommendations on testing were already studied in this thesis. After getting a rectifiable output voltage, the work listed below is recommended.

(1)   Power Conditioning Circuit

Voltage and power efficiency of a full-wave bridge rectifiers with silicon and Schottky diodes and full-wave MOSFET bridge rectifier described in Chapter III should be investigated in a hardware model.

(2)   Array of Devices

According to the platforms, weapon systems, or engines where PEHs are going to be used, the power, voltage, and current needs of a number of devices will vary. The connection geometries investigated in this thesis can be tested for number of devices.

(3)   Cost-Effectiveness Analysis

For single devices, the maximum power output is more important than the cost of the power conditioning circuit, whereas for higher power needs, as the number of devices increases so does the cost. For example, even though having relatively lower voltage and power efficiency, a standard power conditioning circuit that consists of a full-wave silicon diode rectifier and a smoothing capacitor can be better option than a full-wave passive MOSFET bridge rectifier because of its lower cost. A cost-effectiveness analysis is needed determine the optimum method.

(4)   Fatigue Analysis

A log of the accelerometer frequency, amplitude, and duration of the test was kept for the second device during vibrational test. It is recommended to keep the records to

determine the lifetime of the device and to monitor the fatigue over time. Failure analysis described by Householder [1] is also recommended as future work.

(5)   Investigating the Difference between Devices

PEHs used in this thesis and in Householder [1] are both third-generation PiezoMUMPs devices. Although dies are cut from the same wafer, they demonstrate different performances under same test settings. The second device has higher voltage output, and therefore higher power than the initial one. Preparing rest of the third-generation PiezoMUMPs devices and testing them under same conditions will lead to a better understanding for future studies while fabricating an array of devices.

THIS PAGE INTENTIONALLY LEFT BLANK

LIST OF REFERENCES

[1]   T. J. Householder, "MEMS-based waste vibration and acoustic energy harvesters," M.S. thesis, Physics Dept., Naval Postgraduate School, Monterey, CA, 2014.

[2]   D. Hogue and S. Gregory, "MEMS-based waste vibrational energy harvesters," M.S. thesis, Physics Dept., Naval Postgraduate School, Monterey, CA, 2013.

[3]   T. Hehn and Y. Manoli, Eds., *CMOS Circuits for Piezoelectric Energy Harvesters* (Springer Series in Advanced Microelectronics 38)*, Dordrecht, Netherlands, 2015, pp. 21–40.

[4]   C. Liu, *Foundations of MEMS*, 2nd ed. Upper Saddle River, NJ: Prentice Hall, 2012, pp. 269–273.

[5]   C. B. Williams and R. B. Yates, "Analysis of a micro-electric generator for microsystems," *Sensors and Actuators A: Physical.* 52, pp. 8–11, Mar.–Apr. 1996.

[6]   *7600 Plus Precision LCR Meter Instruction Manual*, QuadTech, Maynard, MA, 1997

[7]   N. Kong, D. S. Ha, A. Erturk, and D. J. Inman, "Resistive impedance matching circuit for piezoelectric energy harvesting," *J. of Intelligent Material Syst. and Structures,* vol. 21, pp. 1293–1302, Sept. 2010.

[8]   H. Yu, J. Zhou, L. Deng, and Z. Wen, "A vibration-based MEMS piezoelectric energy harvester and power conditioning circuit," *Sensors,* vol. 14, pp. 3323–3341, 2014.

[9]   E. Lefeuvre, A. Badel, C. Richard, L. Petit, and D. Guyomar, "A comparison between several vibration-powered piezoelectric generators for standalone systems," *Sensors and Actuators A: Physical,* vol. 126, pp. 405–416, February 2006.

10]   J. Dicken, P. D. Mitcheson, I. Stoianov, and E. M. Yeatman, "Power-extraction circuits for piezoelectric energy harvesters in miniature and low-power applications," *IEEE Trans. Power Electron.,* vol. 27, pp. 4514–4529, 2012.

[11]   G. D. Szarka, B. H. Stark, and S. G. Burrow, "Review of power conditioning for kinetic energy harvesting systems," *IEEE Trans. Power Electron.,* vol. 27, no. 2, pp. 803–815, Feb. 2012.

[12]   J. Qiu, H. Jiang, H. Ji, and K. Zhu, "Comparison between four piezoelectric energy harvesting circuits," *Frontiers of Mech. Eng. in China*, vol. 4, pp. 153–159, Jun. 2009.

[13]   D. Maurath and Y. Manoli, Eds., *CMOS Circuits for Electromagnetic Vibration Transducers* (Springer Series in Advanced Microelectronics 49)*,* Dordrecht, Netherlands, 2015, pp. 21–23.

[14]   M. Yilmaz, "Passive full-wave MOSFET rectifiers for electromagnetic harvesting," M.S. thesis, Elect. and Comp. Eng. Dept., University of Waterloo, Waterloo, Ontario, Canada, 2013.

INITIAL DISTRIBUTION LIST

1. Defense Technical Information Center
   Ft. Belvoir, Virginia

2. Dudley Knox Library
   Naval Postgraduate School
   Monterey, California